

# Estimating the amplitude of plastic strain from the distribution of the dislocation morphologies in front of the crack tips

H.L. Huang<sup>a,\*</sup>, N.J. Ho<sup>b</sup>, T.L. Hu<sup>c</sup>

<sup>a</sup> Department of Mechanical Engineering, Chinese Military Academy, Fungshan 830, Taiwan

<sup>b</sup> Institute of Materials Science and Engineering, National Sun Yat-sen University, Kaohsiung 807, Taiwan

<sup>c</sup> Department of Chemistry, Chinese Military Academy, Fungshan 830, Taiwan

Received 9 April 2004; received in revised form 2 July 2004

## Abstract

The purpose of this study is to estimate the amplitude of plastic strain and stress from the dislocation structures in front of fatigue crack tips at various propagation rates in copper. The results are: (1) for both  $5 \times 10^{-5}$  and  $5 \times 10^{-6}$  mm per cycle propagation rates, the maximum plastic strain amplitude is more than  $1.2 \times 10^{-3}$  and the maximum stress amplitude is more than 115 MPa ahead of the crack tips; (2) for  $4 \times 10^{-7}$  mm per cycle propagation rate, the maximum plastic strain amplitude is about  $6 \times 10^{-4}$  and maximum stress amplitude is about 96 MPa; and (3) for a  $2 \times 10^{-8}$  mm per cycle propagation rate, the maximum plastic strain amplitude is about  $7 \times 10^{-5}$  and maximum stress amplitude is about 70 MPa in front of the crack tips.

© 2004 Elsevier B.V. All rights reserved.

**Keywords:** Dislocation; Plastic strain amplitude; Stress amplitude; Crack tip.

## 1. Introduction

For the last several decades, there were many investigations into the dislocation structures of fatigue, especially in metals such as copper [1–3], iron [4], nickel [5] and stainless steels [6]. The dislocation structures in copper are the most clearly defined, no matter the effect by loading condition [7,8], strain amplitude [9,10], temperature [11,12], single crystal [13], polycrystal [14], grain size [15] or frequency [16]. According to Ackermann et al. [2], results of the dislocation structures are dominated by two phases at the plastic strain amplitude location between  $10^{-3}$  and  $10^{-4}$  for single crystals, and that the dislocation structure is dominated by dislocation cells at a plastic strain amplitude larger than  $2 \times 10^{-3}$ . At the same time, Figueroa et al. [17] point out the relationship between dislocation structure and plastic strain amplitude in polycrystals. Based on the above, it is clear that the dislocation structure is dominated by strain amplitude.

However, it is difficult to measure the plastic strain amplitude in front of crack tips, because the plastic strain amplitude varies considerably in a narrow area during the experiment. Huang et al. [18] found that the dislocation structures ahead of crack tips varied in crack propagation rates, through using the electron channeling contrast images [19] with the scanning electron microscope (SEM). Compared to the transmission electron microscopy (TEM), the SEM provides greater advantages, showing the dislocation structure actually ahead of the crack tips, the area of observation is large, and the specimen is easy to prepare. Based on this, it becomes possible to estimate the plastic strain amplitude variation in a small area ahead of the crack tips.

## 2. Experimental

A polycrystalline copper plate of high purity (99.95%) was used for this study. The specimens were annealed at 850 °C for 2 h in a vacuum of  $10^{-5}$  torr and then cooled in the furnace. The grain sizes of the specimens were about 60–80  $\mu\text{m}$ .

\* Corresponding author. Tel.: +886-7-7466641; fax: +886-7-7104697.  
E-mail address: hlhuang@cc.cma.edu.tw (H.L. Huang).

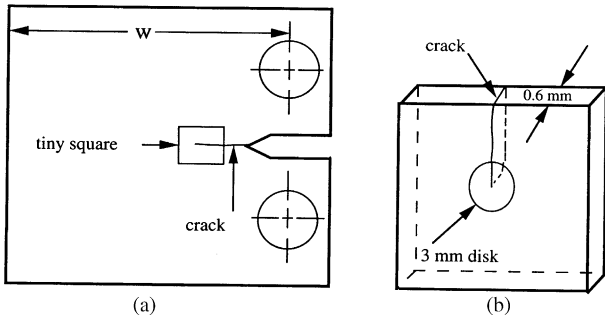
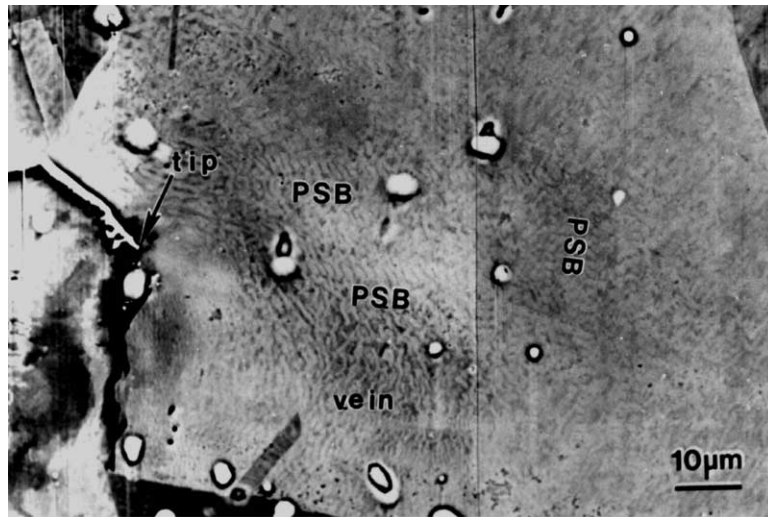


Fig. 1. Schematic diagrams of the foil preparation: (a) position of tiny square; and (b) position of discs.

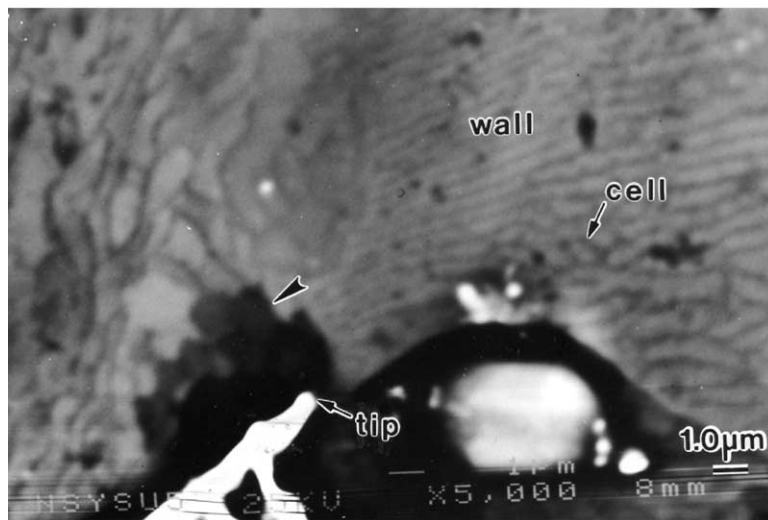
The preparation of specimens followed the instructions of ASTM E647 for single edge compact tension specimens. The crack propagation was induced by a computerized In-

stron 1332 hydraulic testing machine at  $R = 0.1$  (loading ratio,  $R = P_{min}/P_{max}$ ), and at a frequency of 20 Hz. The crack length was measured by a traveling microscope with an accuracy of  $\pm 0.01$  mm. During crack propagation, the crack was allowed to propagate for a length of 0.254 mm at each individual step, while the load was held constant, and the effective loading was then reduced by 5–8% of the previous individual step loading. This procedure was repeated until the rate of crack propagation was reached at which it was intended to study the dislocation structures.

After fatigue crack propagation was completed, the fatigue specimens were cut into squares of 10 mm, each containing a crack with a crack length larger than 3 mm (Fig. 1(a)). The squares were then cut into slices with a thickness of 0.6 mm (Fig. 1(b)) and the slices were ground to a thickness of 0.15–0.2 mm by abrasive paper; finally disks of 3 mm in diameter were punched by Gattan puncher. A smooth sample



(a)



(b)

Fig. 2. The dislocation structure in front of crack tips at a crack propagation rate of  $5 \times 10^{-6}$  mm per cycle. (a) Low magnification; and (b) high magnification (arrow index is misorientation cell structure).

surface after polishing that satisfies the resolution requirement for using back-scatter electron image (BEI) of the SEM was obtained for analysis of the dislocation morphologies. The 3 mm disks were twin-jet polished about one minute time using Struers D2 polishing solution at 5–7 V and 5–10 °C to obtain a smooth sample surface with the crack tip complete. A JEOL 6400 SEM was employed to examine the microstructures in front of the crack tip by means of BEI of SEM at a voltage of 25 KV and a working distance of 8 mm. In order to obtain clearly observable microstructures, the function of rotation and tilt in the SEM were used to adjust the plane of any grain normal to the electronic beam (in zone condition) during the observation.

**3. Results and discussion**

The dislocation morphology around a fatigue crack tip, at a crack propagation rate of  $5 \times 10^{-6}$  mm per cycle, is shown in Fig. 2. Within a 3 μm distance of the crack tip, misorientation cells and the following neighboring dislocation cells extend to 10 μm, each with an average diameter of 0.7–0.8 μm. Next to the cells were different types of walls and persistent slip bands (PSBs) corresponding to the degree of accumulated local plastic strain. Condensed walls occupied an area only 10 μm wide, and then, the PSBs with multiple-directional ladder-like dislocation walls and single-directional ladder-like dislocation walls, occupied the next 50 μm. Outside the ladder-like PSBs, which were located 120 μm away from the crack tip, were vein structures and loop patches corresponding to the very low local plastic strain amplitude that occurs when the fatigue strength nears the fatigue limit.

Based on the results of Figueroa et al. [17] in polycrystals, the dislocation structure is dominated by fatigue cells when the plastic strain amplitude is higher than about  $5 \times 10^{-4}$ . Similarly, the dislocation dipolar wall is found of between 6

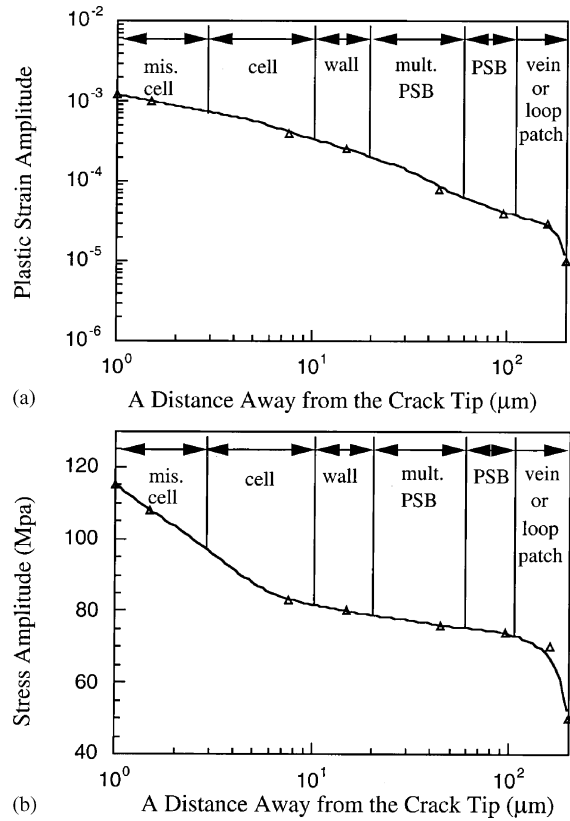


Fig. 3. The evaluation of the amplitude of plastic strain and the amplitude of stress in a small region ahead of crack tips at a  $10^{-6}$  mm per cycle crack propagation rate. (a) Plastic strain; and (b) stress.

$\times 10^{-5}$  and  $7 \times 10^{-4}$ , vein structure exists of between  $3 \times 10^{-5}$  and  $3 \times 10^{-4}$  and the dipolar structure applies at lower amplitudes  $1 \times 10^{-6}$  up to  $6 \times 10^{-5}$ . Basically, it is inaccurate to use the dislocation structure distribution ahead of the crack tips in order to evaluate the amplitude of plastic strain and stress. However, since it is extremely difficult to measure the

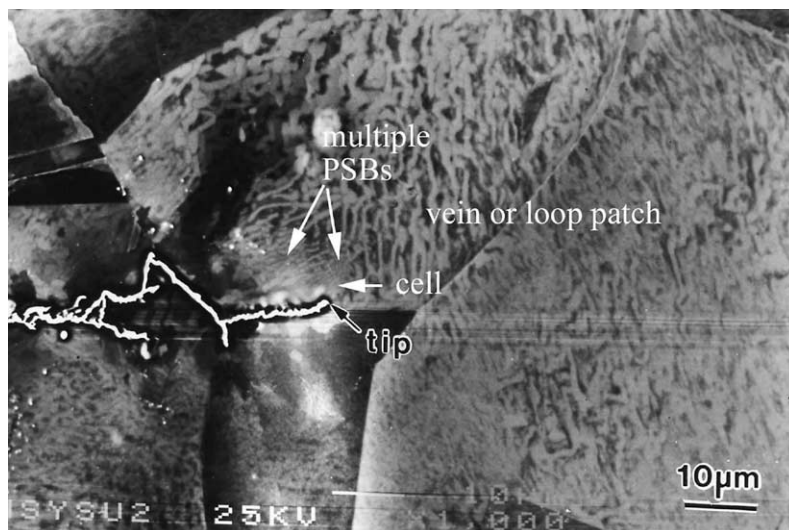


Fig. 4. The dislocation morphologies ahead of the crack tips at a propagation rate of  $4 \times 10^{-7}$  mm per cycle.

amplitude of plastic strain and stress in a small area in front of the crack tips, these results can offer a reference.

According to the dislocation structure in front of the crack tips at  $5 \times 10^{-6}$  mm per cycle propagation rate (Fig. 2(a,b)) and the results of Figueroa et al. [17], the amplitude of the plastic strain (Fig. 3(a)) and the amplitude of the stress (Fig. 3(b)) in a small area, located ahead of the crack tips can be estimated. Therefore, these results (Fig. 3) reveal that the amplitude of the plastic strain is about  $1.2 \times 10^{-3}$ , and that the stress amplitude is 115 MPa within a  $3 \mu\text{m}$  area ahead of the crack tips at a  $10^{-6}$  mm per cycle propagation rate. At the same time, according to the plastic strain amplitude/fatigue life curve obtained by Polák and Klesnil [20], the number of fatigue cycles (fatigue life) is about  $2 \times 10^4$  cycles for the  $1.2 \times 10^{-3}$  plastic strain amplitude (the area is occupied by misorientation cell structure). Similarly, it can be estimated that the fatigue life is about  $1 \times 10^5$  cycles for the cell structure region; about  $1.5 \times 10^6$  cycles for the dislocation wall structure region; about  $1 \times 10^7$  cycles for multiple PSBs structure region and is larger than  $1 \times 10^7$  cycles irrespective of whether the dislocation structure consists of PSBs, vein or loop patches. The estimation of the fatigue life for  $5 \times 10^{-6}$  mm per cycle is larger than that shown by the actual rate of crack propagation in the experiment. This is because the curve of plastic strain amplitude versus number of fatigue cycles [20], obtained by low cycle fatigue, induces the dislocation evolution and crack initiation. This means that the kinetics of dislocation structure development applies as an average and that the plastic strain amplitude is homogenous. However, the dislocation structure is fully developed at the crack tip at  $5 \times 10^{-6}$  mm per cycle propagation rate. In other words, the dislocation morphology is a sequence of misorientation cell, cell, wall, multiple PSBs, PSBs, vein or loop patch structure far away from the crack tips (Fig. 2). These results show that the amplitude of the plastic strain is non-homogenous (decreases with increase

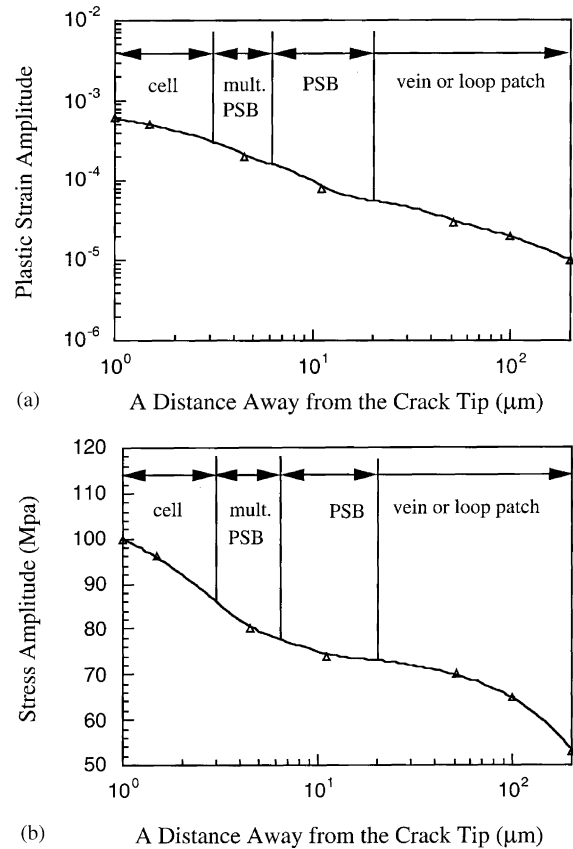


Fig. 5. The evaluation of the amplitude of plastic strain and the amplitude of stress in a small region ahead of crack tips at a  $10^{-7}$  mm per cycle crack propagation rate. (a) Plastic strain; and (b) stress.

in the distance that far away from the crack tips). At the same time, the main structures of the dislocation ahead of the crack tips are walls (amplitude of plastic strain is about  $2 \times 10^{-4}$  and stress amplitude is about 80 MPa) and multiple PSBs (amplitude of plastic strain is about  $1 \times 10^{-4}$

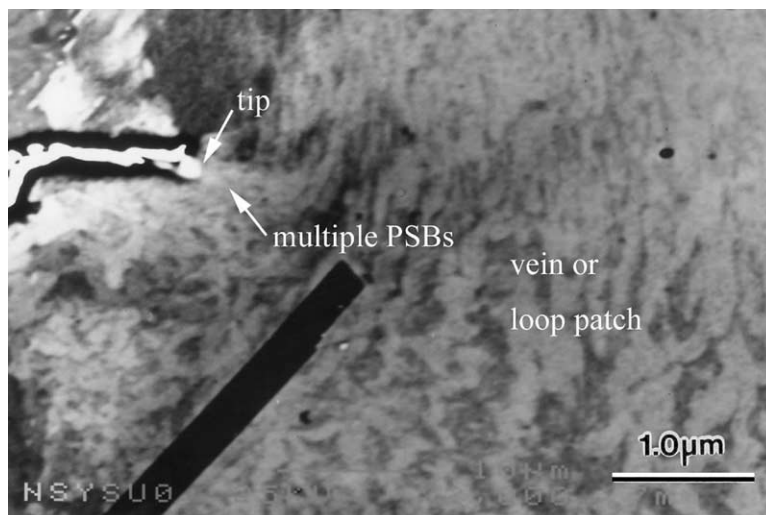


Fig. 6. The dislocation morphologies next to the crack tips at a propagation rate of  $2 \times 10^{-8}$  mm per cycle.

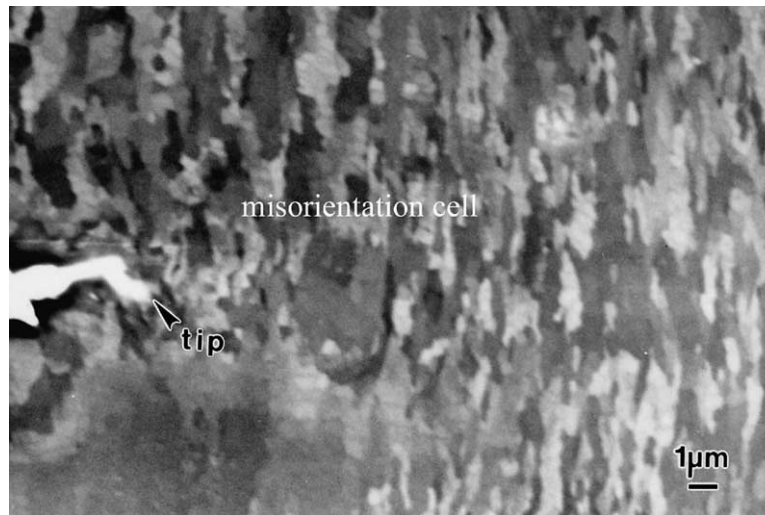


Fig. 7. The dislocation morphologies close to the crack tips at a propagation rate of  $5 \times 10^{-5}$  mm per cycle.

and stress amplitude is about 76 MPa) at a  $5 \times 10^{-6}$  mm per cycle propagation rate. Hence, the misorientation cell structure next to the crack tips is unable to completely determine the rate of crack propagation. In addition, the amplitude of the plastic strain decreases with decreased crack propagation rate. Therefore, this results in a decrease of the fatigue life for the walls and multiple PSBs structure compared to the misorientation cells structure next to crack tips. However, the amplitude of plastic strain increases with decrease in the distance that distance away from the crack tip during the fatigue cracks propagating. Therefore, the real crack propagation rates are larger than the crack propagation rates that were estimated by dominant dislocation structure that are located in front of the crack tips. Based on the above discussion, it is reasonable estimation that the plastic strain amplitude(s) (Fig. 3(a)) and the stress amplitude(s) (Fig. 3(b)) ahead of the crack tips under  $5 \times 10^{-6}$  mm per cycle propagation rate.

For a rate of crack propagation of  $4 \times 10^{-7}$  mm per cycle, the dislocation morphologies in front of crack tips are shown in Fig. 4. The dislocation cells were still limited within a  $3 \mu\text{m}$  range and adjacent multiple PSBs extended to  $3 \mu\text{m}$  in range, and single PSBs occupied the next  $12 \mu\text{m}$ . Veins and loop patches were general elsewhere. Similarly, the plastic strain amplitude (Fig. 5(a)) and the stress amplitude (Fig. 5(b)) in front of the crack tips at a  $4 \times 10^{-7}$  mm per cycle crack propagation rate can be estimated. The results show that the maximum plastic strain amplitude is about  $6 \times 10^{-4}$  and the maximum stress amplitude is about 96 MPa. The dominant dislocation structure is PSBs at a  $4 \times 10^{-7}$  mm per cycle propagation rate (Fig. 4). Therefore, the plastic strain amplitude is about  $8 \times 10^{-5}$  and the stress amplitude is about 75 MPa.

The dislocation morphologies at  $2 \times 10^{-8}$  mm per cycle propagation rate are shown in Fig. 6. The dislocation structure consists of multiple PSBs in a range of about  $3 \mu\text{m}$  next to the crack tips, and from there vein or loop patch structures extend to the next grain. For still lower amplitudes, the dislocation structure is dominated by loop patches at a rate of  $2 \times 10^{-8}$  mm per cycle. On the contrary, for  $2 \times 10^{-8}$  mm per cycle propagation rate, the maximum plastic strain amplitude is about  $7 \times 10^{-5}$  maximum and the stress amplitude is about 70 MPa, and the main plastic strain amplitude is about  $9 \times 10^{-6}$  and the stress amplitude is 45 MPa.

For  $5 \times 10^{-5}$  mm per cycle, misorientation cell dislocation structure appears immediately adjacent to the crack tip, and its range extends to about 20–30  $\mu\text{m}$  (Fig. 7). This structure then connects with cell and wall structure over a large area. The dislocation structure is dominated by cell structure. For  $5 \times 10^{-5}$  mm per cycle, the maximum plastic strain amplitude is more than  $1.2 \times 10^{-3}$ , and the maximum stress amplitude is more than 115 MPa. At the same time, the main amplitude of plastic strain is about  $6 \times 10^{-4}$  and the stress amplitude is 96 MPa.

#### 4. Conclusions

The dislocation structures for varies crack propagation rates were studied by means of a BEI of SEM. At the same time, the structure of the dislocation morphology at the final stage of low cycle fatigue becomes clearly defined, allowing us to estimate the plastic strain/stress amplitude distribution ahead of the crack tips. Conclusions concerning local and general stress strain amplitudes are listed in the following table:

Status	Rate of crack propagation					
	$5 \times 10^{-5}$ mm per cycles	$4 \times 10^{-6}$ mm per cycles	$2 \times 10^{-7}$ mm per cycles	$5 \times 10^{-8}$ mm per cycles		
	Dislocation structure	Dislocation structure	Dislocation structure	Dislocation structure	Dislocation structure	Dislocation structure
Maximum	Misorientation cells	Misorientation cells	Cells	Cells and multiple PSBs	Cells and multiple PSBs	Cells and multiple PSBs
Overall	Misorientation cells and cells	Walls and multiple PSBs	Veins and loop patches	75 MPa	45 MPa	9 $\times 10^{-6}$
	>115 MPa	76–80 MPa	1–2 $\times 10^{-4}$	96 MPa	70 MPa	7 $\times 10^{-5}$
	>1.2 $\times 10^{-3}$	1.2 $\times 10^{-3}$	1–2 $\times 10^{-4}$	6 $\times 10^{-4}$	8 $\times 10^{-5}$	7 $\times 10^{-5}$
	6 $\times 10^{-4}$	1–2 $\times 10^{-4}$	1–2 $\times 10^{-4}$	6 $\times 10^{-4}$	8 $\times 10^{-5}$	7 $\times 10^{-5}$
	96 MPa	76–80 MPa	1–2 $\times 10^{-4}$	96 MPa	75 MPa	45 MPa
	>115 MPa	115 MPa	1.2 $\times 10^{-3}$	115 MPa	96 MPa	70 MPa

*Remarks:* (1) The maximum indicated that the dislocation structure, plastic strain/stress amplitude close to the crack tip. (2) The overall shown that the dislocation structure, plastic strain/stress amplitude is average in front of the crack tip.

## References

- [1] C. Laird, P. Charsley, H. Mughrabi, Mater. Sci. Eng. 81 (1986) 433.
- [2] F. Ackermann, L.P. Kubin, J. Lepinoux, H. Mughrabi, Acta Metall. 32 (1984) 715.
- [3] P. Neumann, Mater. Sci. Eng. 81 (1986) 465.
- [4] Y. Lan, H.J. Kloor, D.L. Holt, Metall. Trans. 23A (1992) 537.
- [5] S. Chen, G. Gottstein, Mater. Sci. Lett. 24 (1989) 4094.
- [6] N.Y. Jin, Chonghua, X. Chen, Acta Metall. 38 (1990) 2141.
- [7] L. Lanes, C. Laird, Mater. Sci. Eng. A161 (1993) 1.
- [8] B. Yan, A. Hunsche, P. Neumann, C. Laird, Mater. Sci. Eng. 79 (1986) 9.
- [9] H.J. Christ, G. Hoffmann, O. Öttinger, Mater. Sci. Eng. A201 (1995) 1.
- [10] L. Buchinger, S. Stanzl, C. Laird, Philos. Mag. 50 (1984) 189.
- [11] J. Bretschneider, C. Holste, W. Kleinert, Mater. Sci. Eng. A191 (1995) 61.
- [12] Z.S. Basinski, A.S. Korbel, S.J. Basinski, Acta Metall. 28 (1979) 191.
- [13] B.T. Ma, C. Laird, Mater. Sci. Eng. A102 (1988) 247.
- [14] C.D. Lu, M.N. Bassim, Philos. Mag. 70 (1994) 591.
- [15] L. Llanes, A.D. Rollett, C. Laird, J.L. Bassani, Acta Metall. 41 (1993) 2667.
- [16] E. Mayer, C. Laird, Mater. Sci. Eng. A914 (1995) 137.
- [17] J.G. Figueroa, S.P. Bhat, R. Dela Veaux, S. Murzenski, C. Laird, Acta Metall. 29 (1981) 1667.
- [18] H.L. Huang, N.J. Ho, W.B. Lin, Mater. Sci. Eng. A279 (2000) 261.
- [19] R. Zauter, H.J. Christ, H. Mughrabi, Philos. Mag. 66 (1992) 425.
- [20] J. Polák, M. Klesnil, Mater. Sci. Eng. 63 (1984) 189.